Calculated and experimental research of VVER-1000 assembly vibration and fretting damage

Dr. Yu. N. Drozdov[1], Dr. Al. A. Tutnov[2], Dr. A. A. Tutnov[3], E. E. Alekseev[4], V. V. Makarov[5], A. V. Afanasyev[6].

[1] IMASH Machine Study Institute named after A.A.Blagonravov of the Russian Academy of Sciences, Moscow ,101990,Kharitonievski side-st., 4, Russia
Tel./fax: (495) 135-30-97, drozdov@imash.ac.ru;

[2,3,4] Kurchatov Institute Russian Research Centre,
Moscow, 123181, Kurchatov sq., 1, Russia
Tel./fax (499) 196-94-22; tutnov-rncki@rambler.ru

[5,6]Experimental and Design Organization "Gidropress",
Podolsk 142103, Ordgonikidze st., 21, Russia
Tel./fax: (499)-502-79-26; makarov@grpress.podolsk.ru

Abstract

The report covers the methods and results of the latest analytical and experimental studies of fretting corrosion and natural vibrations of a VVER-1000 reactor fuel assemblies (FA). The process of fretting-corrosion was investigated using a multi-specimen facility that simulated fragments of fuel rod-to-spacer grid and lower support grid mating units. A computational model was developed for vibrations in the mechanical system of a fuel rod fragment and a spacer grid fragment. A calculational and experimental modal analysis of a FA was performed. Natural frequencies, modes and decrements of FA vibrations were determined and a satisfactory coincidence of analytical and experimental results was obtained. The assessment of fretting-corrosion process dynamics was made and its dependences on operational factors were obtained.

Keywords

VVER-1000 assembly, vibration and fretting damage, empirical model.

Introduction

Under the conditions of vibration corrosion-resistant part made of structural alloys can be subjected to significant damage in the contact area. This kind of damage is generally called fretting-wear or fretting-corrosion. Fretting was first detected in nuclear engineering in the spacer grids of PRTR reactor fuel rods (USA) [1]. Vibrations arise in nuclear reactors due to coolant flow turbulence and pressure pulses. Typical fuel rod vibration frequencies are within the interval of 80 – 150 Hz [2].

The problem of fuel assembly (FA) service life limitation due to fretting that came into view at the end of the 60-ies in the past century had been successfully solved by the beginning of the 80-ies based on the engineering solutions. However, thirty years had passed and the nuclear engineers find the study of fretting of practical interest. This interst stems from the issue of fuel assembly service life extension and reliability enhancement, the way it used to be thirty years ago [3,4].

The damage due to fretting wear [5] depends on the structural and operational parameters. Consequently, the methods of fuel assembly, fuel rod and spacer grid behaviour modeling shall be oriented at the calculation of these parameters.

Experimental study of FA and fuel rod vibration characteristics

The study of vibration characterisitcs of a full-scale FA mock-up was performed in the air at 20°C with load applied with impact hammer and electrodynamic shaker. The study was carried out at a testing rig designed for FA vertical fastening as a two-support beam, loading it with alternating force applied to one of the spacer grids and measuring the driving force and FA vibrational accelerations.

Prior to the tests the FA mock-up was installed into support thimble and loaded with axial compression force. The design of the FA top and bottom fastening units is standard, the value of the longitudinal springing corresponds to FA springing at reactor operational temperature. The vibrational load was applied to fuel rods, spacer grids and FA supports, the FA vibratioal resonce was measured with piezoelectric accelerometers and a 16-channel analyzer and was processed with Pulse LabShop software.

The tests resulted in determination of frequencies , modes and decrements of natural vibrations of FA proper, as well as those of fuel rods within the spacer grid spans. Two main groups of vibrations of FA proper were determined, namely bending and torsional vibrations. The frequency of the first mode of bending vibrations is equal to 5 Hz and the frequency of the first mode of torsional vibrations is equal to 7,5 – 8 Hz.

Apart from the harmonics typical of FA vibrating as a single whole, harmonics with frequencies typical of the monitored span as well as adjacent spans can be observed in the fuel rod vibration spectra. The frequency of fuel rod vibrations in the spacer grid span is first of all defined by the span length and also by the fuel rod linear mass in the span as well as the spacer grid stiffness to angular turn. Fuel rod natural frequencies are within the range of 2 – 3 kHz in the lower 100 mm long span, from 83 to 138 Hz in the 340 mm long spans and from 280 to 380 Hz in the 260 mm span with a lower linear mass. In order to study the spacer grid location effect on the fuel rod natural frequencies in detail, a study of model vibration was performed, the model comprising a fuel rod taken out of a FA and spacer grid fragments. The tests modeled three cases of spacer grid locations: a FA with 15, 13 and 12 spacer grids.

Two kinds of fuel rod positioning in the spacer grid, tight fitting-in and loose fitting-in with a gap were applied.

The results of the studies of a single rod mock-up vibration show that if the length and linear mass of the span and the type of spacer grid cell fitting-in coincide, the natuarl frequencies of a single fuel rod are close to those of a standard fuel assembly. In case there is a gap in the fuel rod-to-spacer grid cell mating unit, the natural frequencies of the fuel rod go down by 9% on the average. At an impact exitation of any fuel rod span the vibrations of the span attenuate as the distance from the excited span increases. The vibrations of the span can only be seen in the amplitude-frequency spectra of adjacent span vibrations and they are not found in distant spans.

Calculational analysis of FA and fuel rod vibrational characteristics

When the natural frequencies of the fuel rod fragments were being calculated with FEM [6], two cases of mathematical model were considered that account for the fuel column structure: a monolithic fuel column and a fuel column that only resists to contraction. In the latter case the fuel column does not resist to tension: axial gaps generate. The former is a stiffer one and produces higher values of the fuel rod fragment natural frequencies as compared to the actual fuel rod fragment and the latter results in smaller values. Besides, neither the possible pellet-to-pellet gaps nor the pellet-to-cladding gaps in actual fuel rods have been considered.

The calculation results of the natural frequencies of the specified fuel rod fragments and experimental data defined for the fuel rod fragments in the air are provided in Table 1.

The values of natural frequencies defined in the experiment basically agree well with the provided calcuational assessments which supports the correctness of the mathematical model of the fuel rod fragment vibrations. For the case of TVS-2 with 12 spacer grids for 4 – 5, the detected low frequencies of 48 – 66 Hz correspond to the frequencies of fuel rod fragment vibrations in adjacent 510-mm spans.

The highest values of natural frequencies in fuel rod fragments correspond to the mathematical model that considers a fuel column as if it were monolithic. It simplifies the finite-element model and the respective calculations are conservative at fretting-wear assessment.

Experimental study of fretting wear in the fuel rod-to-spacer grid cell unit

At the first stage the experimental studies were being carried out in still water at 20°C with two-and three-span specimens that contained fuel rod cladding with pellet simulators, lower support grid simulator and two or three spacer grid simulators. All in all, 18 specimens of two structural designs and various combinations of 100, 255 and 340 mm long spans were tested. The angle of specimen axes varied from 0 to 45 or 90 degrees against the direction of vibration, i.e. specimen longitudinal and transversal vibration was excited. Figure 1 provides the model and the specimens on the outside. The model is a plate with organic glass cover, suspended vertically from the springs above the shaker. Fuel rod specimens were fastened on the plate. Submerged accelerometers were attached to the fuel rod specimens. The plate was covered with the cover, filled up with water and was attached to the shaker. The tests comprised 8 stages 50 – 55 hours long, the amplitude and frequency of vibrations being maintained the same within each stage. As every stage was completed, the transversal backlash was measured in the fuel rod-to-spacer grid mating unit which could indirectly indicate the beginning of the

wear process. If no new indications of backlash were found, the amplitude or vibration frequency was increased twice at the next stage. The vibration test parameters of the stages varied within the following ranges: the frequency of sine-shaped vibrations within 16,5 – 99 Hz, the amplitude of vibration accelerations within 1 – 25 m/s^2 , test duration was about 50 hours.

Following stages 6 – 8, when transverse backlash appeared in the fuel rod-to-spacer grid unit and traces of vibrational wear were detected in the fuel rod-to-spacer grid cell bulge contact area, roughness measurement of claddings and measurement of the cell inscribed diameters in specimens with the largest backlash had been realized . Based on the results of the measurements curves of cladding wear depth versus the vibrational acceleration amplitude were plotted as well as the curves of increment of the cell inscribed diameter versus the number of vibrational loading cycles (Fig.2). Fig.2 shows that cladding wear starts at spacer grid cells and the fuel rod vibration amplitudes for a 100-mm span within the ranges from 14 – 17 to 22 – 25 m/s^2, for the 340 mm span – from 37 to 57 m/s^2. The maximum depth of fuel rod cladding wear was about 30 μm.

The inscribed diameter of the spacer grid cells increased by 0,1 mm on the average. The maximum diameter increment occured at stages 5 and 6 at amplitudes of about 16 m/s^2, and later on irrespective of vibration amplitude increase, the rate of increment decreased 15 times.

Experiments similar to the above ones were carried out at operating temperatures, pressure, chemical composition of coolant at a special tesing rig within 750 hours [5]. Fuel rod mock-ups with different gaps and fitting-in tightness in the cladding-to-spacer grid cell contact area were tested. The amplitude of vibrational acceleration for different mock-ups varies within the range of 5 – 30 m/s^2. The total number of mock-ups tested was 18. Only one mock-up ended up with a 300 μm deep cladding wear. The mock-up was tested at amplitude of vibrational accelelration of about 30 m/s^2 and vibration frequency 32 Hz. The original diametral gap in the cladding-to-spacer grid cell contact area was 0,1 μm. The other specimens showed no cladding wear that would exceed the unevenness of the surface roughness.

Fuel rod cladding-to-spacer grid fretting wear in the contact area empirical model development

An empirical model of fuel rod cladding-to-spacer grid fretting wear in the contact area was developed based on the experimental data investigation. For the case of wear due to fuel rod transverse vibrations the experimental data confirm the susceptibility to fretting wear of those fuel rod-to-spacer grid mating units where the tight fitting-in has loosened with gap generation. It confirms that even at minimum contact pressures fretting wear is considerably less that in the presence of a gap between the colliding parts. In this respect the model that describes the wear of the cladding and the bulging requires equations that describe the change of the contact forces in the presence of initial tight fitting-in as well as the kinetic equations of tight fitting-in loosening and diametral gap formation. If a fuel rod is installed with the initial tight fitting-in $\Delta<0$ into a spacer grid cell, then for elastic-plastic material behaviour the contact force on the cladding in the area of each bulge can be described in the expression:

$$P_k = 0 \text{ at } \Delta \geq 0;$$

$$P_k = -P_R\left[1-\exp\left(-\frac{K|\Delta|}{2P_R}\right)\right] \text{ at } \Delta < 0,$$

where: P_R – an absolute value of the limiting possible contact force acting by the bulge on the cladding under the conditions of the developed plastic deformation of the bulge; K – stiffness of spacer grid cell bulges, defined in a calculation and depending on material properties and spacer grid cell geometry.

The actual elastic tight fitting-in that remains after fuel rod installation into the spacer grid cell with account for the plastic deformations received by the bulge will be represented as follows:

$$\Delta_y = 0 \text{ at } \Delta \geq 0;$$

$$\Delta_y = -2\frac{P_R}{K}\left[1 - \exp\left(-\frac{K|\Delta|}{2P_R}\right)\right] \text{ at } \Delta < 0.$$

In the course of operation the fitting-in tightness will decrease due to stress relaxation in the bulge. Besides, there will be an increase in the inscribed circumference diameter of the spacer grid cell due to cyclic load caused by fuel rod vibration. The change of tight fitting-in (gap) in time can be defined by an equation:

$$\Delta_t = \Delta_y + \int_0^t d\Delta_{VN}, \quad (1)$$

where $d\Delta_{VN} = d\Delta_V + d\Delta_N + d\Delta_D$; $d\Delta_V$ – change of fitting-in tightness due to stress relaxation in the bulge; $d\Delta_N$ – tight fitting-in (gap) variation due to an increase in the spacer grid cell inscribed circumference diameter resulting from cyclic load caused by fuel rod vibration. $d\Delta_D$ – tight fitting-in (gap) variation due to a change in cladding diameter caused pressure differential under the conditions of thermal and irradiation creep is defined in a calculation with computer codes that model the fuel rod thermal and irradiation mechanics.

To calculate the tight fitting-in (gap) variation due to a change in vibration-induced cell diameter increase we assume the correlation: $d\Delta_N = k\nu dt$, where: k – factor of vibration-induced diameter increase rate that depends on the contact force amplitude (as the first approximation this correlation will be considered linear); ν – frequency of contact force variation, i.e. the frequency of fuel rod vibration in the grid-to-grid span.

The contact force in the support is proportional to fuel rod bowing in the middle of the span between the supports and is inversely proportional to the span length to power 3. In its turn, at harmonic vibrations the bowing amplitude in the middle of the span between the supports is linearly connected with acceleration amplitude in the point with the same coordinate by coefficient $1/(2\pi\nu)^2$.

Consequently, the expression for $d\Delta_N$ can be defined in the form

$$d\Delta_N = q\frac{a_\nu}{\nu}dt, \quad (2)$$

where: $d\Delta_N$ in mm; q – experimentally defined coefficient; a_ν – acceleration amplitude in the middle of the span, m/s^2; ν – fuel rod vibration frequency, Hz.

It is worth mentioning that in the course of the experiments in 2005 during the initial six stages of loading with acceleration amplitude increased at each one, there were no traces of fretting-wear in the claddings and bulges exceeding the surface roughness. However, a gap generated within this period of time. Since the tests were performed at 20 °C, the thermal creep at the temperature can be neglected and there was no irradiation, the component $d\Delta_V$ in equation (1) that characterizes the decrease in fitting-in tightness due to stress relaxation is close to zero. Similarly, component $d\Delta_D$ connected with the change of the fuel rod outside diameter is neglible small. Consequently, once we know the value of the gap generated within 6 stages of the tests, we can choose coefficient q, that characterizes the rate of cell diameter vibration-induced increase. If we apply in expression (2) acceleration in m/s^2 and frequency in Hz, coefficient q will be equal to $5{,}2\cdot10^{-5}$. At this, the value of cell diameter increase will be in mm. This value of coefficient q received to spacer grid cells with a short bulge. To get the values of q for the spacer grid cells of other designs similar experimental studies shall be performed.

The value of fitting-in tightness variation due to stress relaxation in the spacer grid cell is assessed by three-dimensional modeling of fuel rod and spacer grid cell deformation with the finite element method.

Now we pass to deducing the dependence for cladding wear rate under the conditions of fuel rod transverse vibrations. The model will be based on Preson hypothesis [7] that wear in an assigned point is proportional to the work of friction forces on the element surface that contains the point [1]. Then the rate of cladding wear depth variation will be defined the following way:

$$\frac{dh}{dN} = \frac{dh}{\nu\, dt} = \xi f_f \frac{R_k}{S} U\,, \tag{3}$$

where: h – wear depth; dN – number of loading cycles; ξ – coefficient that characterizes wear rate; f_f – friction coefficient; R_k – contact force acting along the normal on the cladding on the part of the bulge; S – bulge-to-cladding contact area; U – tangential motion of cladding with respect to the bulge; ν – frequency of fuel rod vibration-induced oscillations in the spacer grid-to-spacer grid span.

Friction coefficient f_f, according to the classical theory, does not depend on the size of the plateau the contact force is applied to. However, in case the contact area is small, this rule is violated. Strictly speaking, sliding friction transforms into friction of "ploughing" as the contact pressure increases. At this, the friction coefficient can increase several times. The correlation of the value of friction coefficient versus contact pressure can be described in terms of expression: $f_f = f_{\mathrm{Zr}}\left(1 + AP_k^n\right)$, where: f_{Zr} – sliding friction coefficient for zirconium against zirconium friction pair, for zirconium components covered with oxide film the sliding friction coefficient depends on the friction path and can increase several times in the course of film wear out; $P_k = R_k / S = R_k / \left(l_P g\right)$ – contact pressure; S – bulge-to-cladding contact area; l_P – bulge length; g – contact area width; A, n – coefficients, defined experimentally with special hardware.

The values of g increase as the cladding wear depth increase. The correlation of g versus wear depth can be concluded from geometry analysis. Having assumed that in case of no wear the contact area

width is close to zero, and the bulge geometry is plotted as a parabola: $y = \gamma x^2$, following simple transformations the following expression for contact area width can be obtained:

$$g = \frac{2}{\sqrt{\gamma}}\sqrt{R_в - H + \frac{1}{2\gamma} + \sqrt{\left(R_в - H + \frac{1}{2\gamma}\right)^2 + H(2R_в - H)}}$$

where: g in mm; $R_в$ – bulge radius; γ – bulge geometry coefficient; $H = h(1+\mu)10^{-3}$; h – cladding wear depth; μ – bulge wear rate-to-cladding wear rate ration.

Coefficient ξ in (3) is assumed to depend on parameter ω that characterizes the level of accumulated cyclic damage. Parameter ω is an integral taken around the accumulated number of loading cycles-to-damaging number of cycles ratio. It will indirectly account for fatigue damage accumulation in the cladding material and the effect of accumulated damage on the material wear resistance.

The damaging number of cycles N_p can be linked with the amplitude of stress variation $\Delta\sigma$ with a Wailler function: $\Delta\sigma = M(N_p)^{-\beta} + \sigma_{-1}$, where: σ_{-1} – endurance strength; M, β – experimentally defined coefficients.

Here we should refrain from the temptation to define coefficients σ_{-1}, M, β on the basis of a direct transformation of fatigue curve as the structural parameter of capacity to be damaged ω, that controls the decrease in the rate of wear resistance, will not necessarily coincide with the parameter that controls the damage process at cyclic loading. In this respect value σ_{-1} shall be considered as the threshold of material sensitivity to wear based on the level of stresses available in the surface layer, not as the endurance strength. Stress amplitude is proportional to the amplitude of contact pressure variation $K\Delta\sigma = DR_k/S$. With account for the above, we obtain:

$$\xi = \xi_1\left(\int_0^t \frac{\dot{N}}{N_p}d\tau\right)^\eta = \xi_2\left[\int_0^t \nu\left(\frac{BR_k}{S} - \sigma_{-1}\right)^{1/\beta} d\tau\right]^\eta$$

where: $N = \nu t$ – number of contact force variation cycles; ν – fuel rod vibration frequency in a single grid-to-grid span; t – time; S – bulge-to-cladding contact area; ξ_1, ξ_2, B, η, β – experimentally defined coefficients.

Let us consider the relation of contact force R_k and the motion at cladding sliding transverse to the bulge symmetry axis with fuel rod transverse vibration parameters. Let the vertical plane the fuel rod vibrates in, makes angle α with bulge symmetry angle (Figure3).

The amplitude of motion in the spacer grid cell can be presented as the motion amplitude of the middle of a double grid-to-grid span of a fuel rod. Having denoted the amplitude by υ, we resolve it into components along and transverse to the symmetry axis of the bulge: $\upsilon_r = \upsilon|\cos\alpha|$, $\upsilon_\theta = \upsilon|\sin\alpha|$.

Since in experimental studies of fuel rod vibrations, as a rule, acceleration amplitude is recorded in the middle of the spans, we shall define motions υ_r and υ_θ with it considering the harmonic nature of a particular vibration mode: $\upsilon_r = a_D|\cos\alpha|/(2\pi\nu_D)^2$ и $\upsilon_\theta = a_D|\sin\alpha|/(2\pi\nu_D)^2$, where: a_D – amplitude of vibration accelerations in the middle of a double span for the mode of vibration at frequency ν_D, corresponding to span $2L$; L – distance between the middle planes of spacer grids.

The fuel rod motion in a spacer grid cell is limited by the value of diametric gap. So the amount of fuel rod slip in the cell transverse to the bulge symmetry axis in equation (3) will be equal to the smaller value out of the two ones: diametric gap and motion range transverse to the bulge symmetry axis: $U = \min[\Delta,\, a_D|\sin\alpha| / (2\pi\nu_D)^2]$.

It is worth mentioning, that having assumed the hypothesis on the harmonic nature of vibrations, acceleration in the middle of the double span a_D can be written in terms of acceleration of the middle of a single span: $a_D = \sqrt{2}\, a_\nu$, where: a_ν – acceleration in the middle of a single span with vibration mode typical of double span. Then we have $U = \min[\Delta,\, a_\nu|\sin\alpha| / (\sqrt{2}\pi^2\nu^2)]$.

If along with transverse vibrations axial vibrations are observed in a fuel assembly, function U shall be replaced by expression: $U_{zz} = \sqrt{U^2 + U_z^{\,2}}$ where: $U_z = a_z/(2\pi\nu_z)^2 - U_g$; a_z, ν_z – acceleration and frequency of fuel rod longitudinal vibrations, U_g – axial motion of grid in the area of a particular fuel rod installation due to the action of friction forces in all cells. The value of U_g is calculated at modeling fuel assembly longitudinal vibrations considering the possibility of fuel rod slip in the spacer grid cells.

At fuel rod vibrations depending on the correlation of diametric gap and fuel rod vibration amplitude in the spacer grid cell the cladding will collide with one or several bulges. At this, the contact force acting on the cladding on the part of the bulge R_k, will be proportional to fuel rod bowing in the middle of a single span υ_r and reversely proportional to span length to power 3: $R_k = Ba_\nu(2\pi\nu)^{-2} L^{-3}|\cos\alpha|$, where: a_ν – acceleration in the middle of a fuel rod single span L for the mode of single span vibration at frequency ν; B – coefficient.

The rate depends on the azimuth of direction fuel rod vibrates in, which changes every time it has collided with a bulge. With $\Phi(\alpha)$ to denote the probability density of vibration vector (angle α), the expression for the averaged wear rate considering the random nature of vibration direction distribution will be as follows:

$$\frac{dh}{dt} = \zeta \int_0^{\pi} \Phi(\alpha)\nu P_k \xi_2 \left[\int_0^t \nu (BP_k - \sigma_{-1})^{1/\beta}\, d\tau \right]^{\eta} (1 + AP_k^n) \min\left[\frac{\Delta,}{\dfrac{a_\nu|\sin\alpha|}{\sqrt{2}(\pi\nu)^2}} \right] d\alpha, \qquad (4)$$

where $P_k = a_\nu|\cos\alpha| / [L^3 \nu^2 l_P g(h)]$.

The random nature of hydrodynamic excitation loads at longitudinal-transverse coolant flow, fuel rod collisions at different angles with respect to the bulge symmetry axis and resulting continuous changes of the direction of fuel rod jumps bring about the uniform distribution of angles that define the direction of fuel rod vibration: $\Phi(\alpha) = 1/\pi$

When creating the fretting-wear model, the appearance of hard oxide film on the cladding surface within the first few hours of fuel rod operation in a VVER-type reactor or within the first few hours of testing in an autoclave at a temperature above 300 °C shall be taken into consideration.

The film is about 5 μm thick. In the course of fuel rod operation, cladding oxidation results in surface film thickness growth. Consequently, two competing processes take place simultaneously: oxide

film thickness growth due to oxidation and its reduction caused by fretting wear in the places of its contact with the spacer grid. The differential equation for the kinetics of oxide film thickness in the contact area is written as follows: $\partial\delta / \partial t = F_1(T,\delta) - F_2$ on initial condition of $\delta(\tau = 0) = 5$ μm, where δ is the oxide film thickness, τ is the time, $F_1(T,\delta)$ is the rate of oxide film growth thickness, depending on the temperature T and the thickness of film proper, F_2 is the rate of oxide film wear out. Function $F_1(T,\delta)$ for zirconium alloys is known to look as follows: $F_1(T,\delta) = F_0 \exp(-T_0/T)/2\delta$, where F_0, T_0 – constants, T – temperature.

So far, it is not clear whether the film further generated is as hard as the one initially generated. In this respect we conservatively assume that the thickness of initially generated hard film does not grow.

With account for the presence of hard oxide film with thickness h_0, correlation (4) can be rewritten as follows:

$$h = \begin{cases} \Psi_1 & at\ h < h_0, \tau < t_0; \\ h_0 + \Psi_2 & at\ h \geq h_0, \tau \geq t_0 \end{cases} \qquad (5)$$

where $\Psi_i = \zeta_i \int_{\tau_0}^{\tau} \int_0^{\pi} \nu P_k \left[\int_0^t \nu \left(B_i P_k - \sigma_i \right)^{1/\beta_i} d\tau \right]^{\eta_i} \left(1 + A_i P_k^{n_i}\right) \min\left[\frac{\Delta,}{\frac{a_\nu |\sin\alpha|}{\sqrt{2}(\pi\nu)^2}} \right] d\alpha\, dt$, $i = 1, 2$;

$P_k = a_\nu |\cos\alpha| / \left[L^3 \nu^2 l_P g(h) \right]$; $\tau_0 = 0$ at $i = 1$, $\tau_0 = t_0$ at $i = 2$; t_0 – time at $h = h_0$.

14 experimentally determined constants: $\zeta_1, \zeta_2, B_1, B_2, \sigma_1, \sigma_2, \beta_1, \beta_2, \eta_1, \eta_2, A_1, A_2, n_1, n_2$ are present in provided correlations for wear depth. Evidently, the results of not less than twelve experiments on cladding wear depth definition shall be available to define them. Unfortunately, the available database on both operational and testing bench results for cladding wear, in most cases provides indirect and insufficiently precise data on wear depth. Three experiments can only be pointed out with wear depth estimated using section metallographic study. In particular, in the course of two experiments performed in OKB "Gidropress" testing bench referred to in the beginning of the article, having tested the specimens for about 50 hours at loading stage 7 and for the same time at loading stage 8 at 20 °C and at different levels of acceleration amplitude and vibration frequencies, the wear depth was determined equal to 10 and 30 μm, respectively. Besides, in experiments at temperature close to operating, the fuel rod cladding wear depth of 300 μm for 750 hours of testing was recorded in one specimen. In all the other cases we deal with either mentioning of wear without indicating its depth, or with wear signs within surface roughness, or no wear at all.

Under the circumstances, the search of the 14 unknown coefficients in equations (5) can only be realized by linear programming method with determination of the minimum of Φ function below: $\Pi = \sum_{i=1}^{N} \rho_i(h_i, \overline{h_i})$, where: $h_i, \overline{h_i}$ – rated and experimentally determined wear depth, $\rho_i(h_i\, \overline{h_i}) = (h_i - \overline{h_i})^2$ for experiments in which the wear depth was determined for the metallographic sections.

For the experiments in which the wear depth was not determined by metallographic method, function ρ_i will be written as follows:

$$\rho_i(h_i\,\overline{h_i}) = \begin{cases} 0 \ at\ \overline{h_{i1}} \le h_i \le \overline{h_{i2}} \\ \left[h_i - \overline{h_{i1}}\right]^2 \ at\ h_i < \overline{h_{i1}} \\ \left[h_i - \overline{h_{i2}}\right]^2 \ at\ \overline{h_{i2}} < h_i \end{cases},$$

$\overline{h_{i1}}$, $\overline{h_{i2}}$ are the limits of possible wear depth set up by an expert on the basis of the data available in the test reporting documents that specify oral explanations of the specialists engaged in performing the experiments. In case the reporting documents indicate no wear, $\overline{h_{i1}}$ is assumed to be equal to zero, and $\overline{h_{i2}}$ to be equal to the maximum height of the rough surface dents.

Despite a sufficiently high effectiveness of the above approach to a search of the unknown coefficients in the cladding wear equations, the available experimental database is not enough to create a complete mathematical model with fourteen coefficients that characterize the material resistance to wear. Along with the three experiments mentioned above, only two more experiments contain totally new information on lack of traces of cladding wear after tests in hot and cold states. We can conservatively assume for one experiment in the series with maximum loading level and no traces of wear the wear depth equal to the height of rough surface texture. The other experiments either to a certain extent repeat the information obtained in the above five experiments or do not provide reliable data on the cladding wear depth.

In this respect the number of unknown coefficients needs to be decreased by reducing the effects accounted for in the created model. Thus, having assumed coefficients A_1 and A_2 equal to zero, we will not consider the dependence of friction coefficient on the contact force, i.e. the effect of run-in setting in the cladding-to-bulge contact area. At this, there will automatically be no need in defining coefficients n_1 and n_2, since the multiplier they are incorporated in will be multiplied by zero. Let us also assume that in the transverse section the bulge is sufficiently obtuse and in the process of bulge and cladding wear the contact spot width does not change $g(h) = const$.

Besides, let us conservatively assume the threshold of material sensitivity to wear by the level of stresses σ_{-1} equal to zero.

It will result in only six unknown coefficients in the model, and formulae (5) take the form:

$$h = \begin{cases} \Psi_1 & \text{при } h < h_0, \tau < t_0; \\ h_0 + \Psi_2 & \text{при } h \ge h_0, \tau \ge t_0 \end{cases} \qquad (6)$$

where $\Psi_i = \dfrac{\zeta_i}{\left(L10^{-3}\right)^{3(1+\lambda_i\eta_i)}\left(l_P 10^{-3}\right)^{1+\lambda_i\eta_i}} \int_{\tau_0}^{\tau} \frac{a_\nu}{\nu} \int_0^{\pi} |\cos\alpha| \left[\int_0^t \nu \left(\frac{a_\nu |\cos\alpha|}{\nu^2}\right)^{\lambda_i} d\tau\right]^{\eta_i} \min\left[\frac{\Delta,}{10^3 a_\nu |\sin\alpha|}{\sqrt{2}(\pi\nu)^2}\right] d\alpha\, dt$, i= 1,2;

$\tau_0 = 0$ at $i = 1$, $\tau_0 = t_0$ at $i = 2$; t_0 – time at $h = h_0$; L, l_p – in mm; a_ν – m/s^2.

The processing of experimental database with linear programming method provided the following values of coefficients in formulae (6) ζ_1=2,2·10^{-17}, ζ_2=2,48·10^{-12}, λ_1=1,66, λ_2=1,5, η_1=1,3, η_2=1,4.

The calculation assessments with the obtained formulas show that under the conditions of fuel rod operation as a part of fuel assemblies in VVER-1000 reactor cores at typical values of vibration accelerations 1,5 m/s^2 and fuel rod vibration frequency 74 Hz for 1500 days, in case of 0,1 mm initial

tight fitting-in of the fuel rod-to-spacer grid mating unit, the cladding wear depth is 10^{-5} μm. In case the initial tight fitting-in is 0,01 mm under the same loading parameters, the wear depth is 0,2 μm.

References

1. Уотерхауз Р. Б., Фреттинг-коррозия. Л., Машиностроение, 1976.
2. Paidossis M., A review of flow-induced vibrations in reactor components. Nucl. Eng. and Design, 1983, v.74, N1, pp. 31-60
3. Драгунов Ю. Г., Дроздов Ю. Н., Макаров В. В., Влияние сил трения на работоспособность и ресурс тепловыделяющих сборок водоводяных энергетических реакторов, Трение и износ, Ин-т механики металлополимерных систем им. В.А. Белого НАН Беларуси, Беларусь, Гомель, 2006, т. 27, н. 1, январь-февраль, стр. 54 – 60
4. Brown C., Adams F., Cooke G., Fuel rod vibration and fretting impact on reliability, – In: the 2004 Intern. Meeting on LWR Fuel Performance, Orlando, Florida, September 19 – 22, 2004, Paper 1059.
5. Ko P., Wear of zirconium alloys due to fretting and periodic impacting. In: Ludema K. et al. Wear of Materials 1979, N. Y. , ASME, 1979, pp. 388–395.
6. Зенкевич О., Метод конечных элементов в технике, М., Мир, 1974, 341 стр.
7. Цеснек Л. С., Механика и микрофизика истирания поверхностей, М., Машиностроение, 1979, 264 стр.

Table 1. The experimental data ahd calculation results of the natural frequencies of the specified fuel rod fragments

Experiment	Natural frequencies, Hz	
	Experiment	Calculation[1]
9 fuel rod fragment simulators [2]	72	68 – 88
15 spacer grid TVS-2 fuel assembly[3], all spans 255 mm long	140 – 260	202 – 259
12 – spacer grid TVS-2 fuel assembly [3], spans and longs:		
1 – 2 and 2 – 3 at 255 mm	140 – 260	202 – 259
4 – 5 at 255 mm	48 – 66 and 140 – 260	202 – 259
7 – 8 at 510 mm	48 – 66	50 – 64
4 – 5 at 255 mm	140 – 260	202 – 259
TVS-2M [3], spans 340 mm long	90 – 150	113 – 146

[1] first - a fuel column that only resists to contraction, second - a monolithic fuel column
[2] OKB “Gidropress” testing bench in 2002
[3] Experimental studies of natural frequencies of a single fuel rod model at OKB Gidropress in 2005

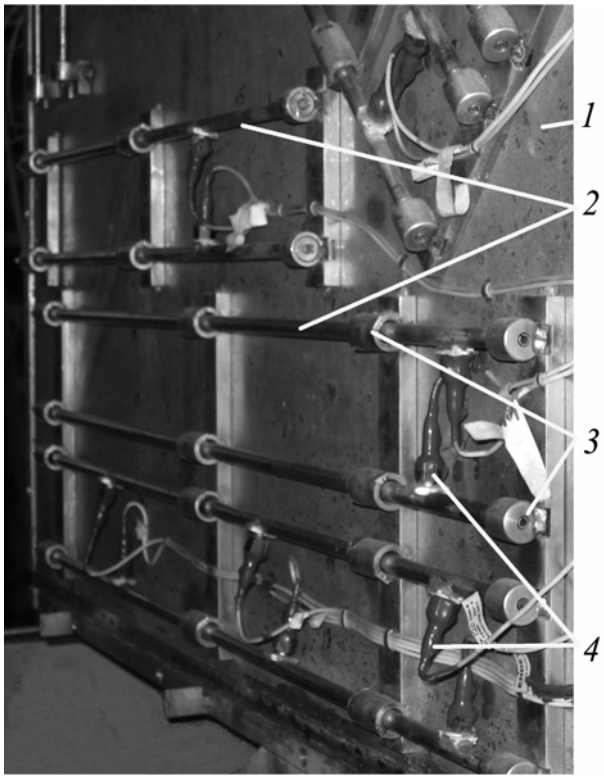

Figure 1. Model for fretting-wear testing: 1 – plate; 2 – two-and three-span specimens that contained fuel rod cladding with pellet simulators; 3 – spacer grid simulators; 4 – accelerometers

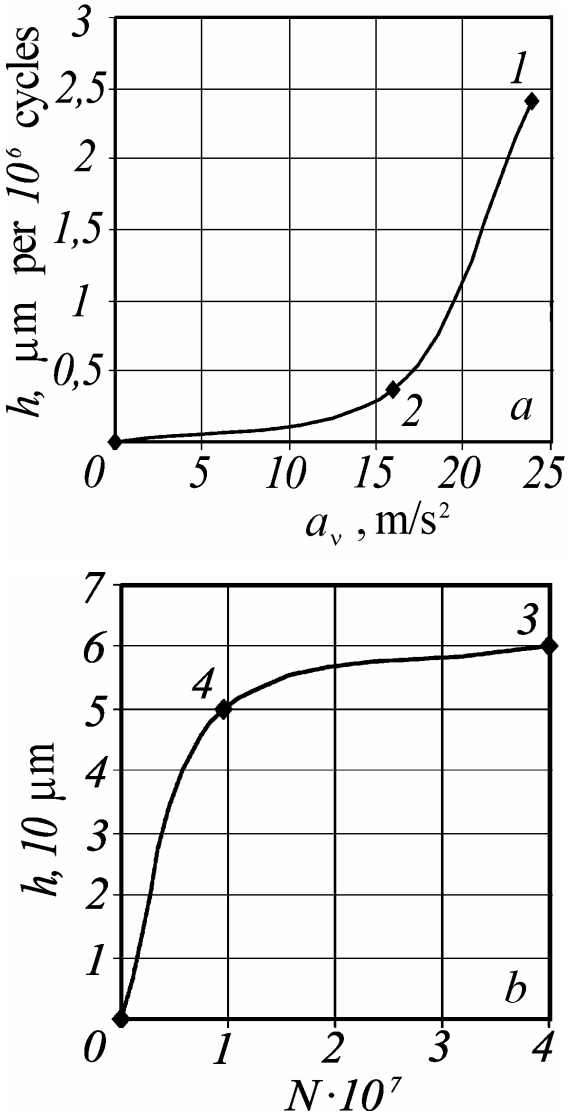

Figure 2. Correlation of cladding wear depth versus vibration acceleration amplitude (a) and bulge wear depth versus the number of cycles (b): 1, 2 – wear at Stage 8 (amplitude = 22 – 25 m/s^2, τ = 52 h 20 min, amplitude in 340 mm span up to 57 m/s^2) and 7 (amplitude = 14 – 17 m/s^2, τ = 50 h 45 min, amplitude in 340 mm span up to 37 m/s^2); 3, 4 – after Stages 5 – 8 (amplitude = 14 – 25 m/s^2, τ = 208 h 35 min) and Stages 5 – 6 (amplitude = 16 m/s^2, τ = 105 h 30 min)

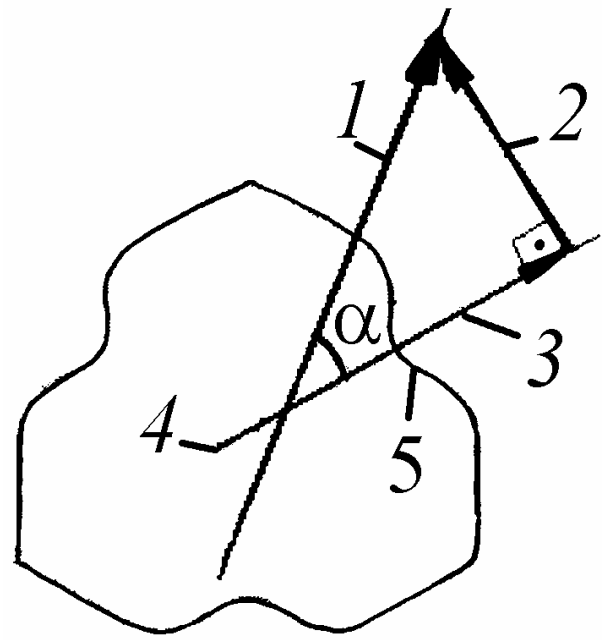

Figure 3. Fuel rod vibration diagram: 1 – direction of fuel rod vibration; 2 – υ_θ, 3 – υ_r – azimuthal and radial fuel rod vibration amplitudes; 4 – bulge symmetry axis; 5 – bulge.